*Supplementary information*

# Formation of Nanofoam carbon and re-emergence of Superconductivity in compressed $CaC_6$

Yan-Ling Li,[1] Wei Luo,[2] Xiao-Jia Chen,[3,4] Zhi Zeng[4] , Hai-Qing Lin[5] & Rajeev Ahuja[2,6]

[1] School of Physics and Electronic Engineering, Jiangsu Normal University, 221116, Xuzhou, People's Republic of China

[2] Condensed Matter Theory Group, Department of Physics and Astronomy, Uppsala University, P.O. Box 516, SE-751 20 Uppsala, Sweden

[3] Geophysical Laboratory, Carnegie Institution of Washington, Washington, DC 20015, USA

[4] Key Laboratory of Materials Physics, Institute of Solid State Physics, Chinese Academy of Sciences, Hefei 230031, People's Republic of China

[5] Beijing Computational Science Research Center, Beijing 100089, People's Republic of China

[6]Applied Material Physics, Department of Materials Science and Engineering, Royal Institute of Technology (KTH), SE-100 44, Stockholm, Sweden

**This file includes Three Tables and nine Figures.**

**Supplementary Table S1. Structures of stable phases of $CaC_6$ and carbon foam.** Only the fractional coordinates of symmetry inequivalent atoms are given. For *C222* phase, under pressure, it is easy to transform into *Cmmm* symmetry, which is verified by total enthalpy calculation.

| Pressure (GPa) | Space group ( No. ) | Lattice parameters $(a, b, c, \alpha, \beta, \gamma)$ ( $\AA$, $^0$ ) | | | Atomic fractional coordinates | | | |
|---|---|---|---|---|---|---|---|---|
| 0 | *R-3m* | 5.1683 | 5.1683 | 5.1683 | Ca 4*i* | 0.0000 | 0.0000 | 0.0000 |
| | (164) | 49.7 | 49.7 | 49.7 | C1 6*g* | 0.1667 | 0.8333 | 0.5000 |
| 19 | *C222* | 9.1472 | 3.6947 | 3.5964 | Ca 2*a* | 0.0000 | 0.0000 | 0.0000 |
| | (29) | 90 | 90 | 90 | C1 4*f* | 0.4213 | 0.0000 | 0.5000 |
| | | | | | C2 8*l* | 0.1751 | 0.8082 | 0.4999 |
| 39 | *Pmmn* | 5.8904 | 2.4893 | 6.4903 | Ca 2*b* | 0.0000 | 0.5000 | 0.7425 |
| | (59) | 90 | 90 | 90 | C1 2*b* | 0.0000 | 0.5000 | 0.3159 |
| | | | | | C2 2*a* | 0.0000 | 0.0000 | 0.1766 |
| | | | | | C3 4*f* | 0.1994 | 0.0000 | 0.0286 |
| | | | | | C4 4*f* | 0.2791 | 0.0000 | 0.5537 |
| 126 | *Cmcm* | 2.3828 | 16.1113 | 4.0533 | Ca 4*c* | 0.0000 | 0.4874 | 0.2500 |
| | (63) | 90 | 90 | 90 | C1 8*f* | 0.0000 | 0.1044 | 0.4303 |
| | | | | | C2 8*f* | 0.0000 | 0.2705 | 0.5647 |
| | | | | | C3 8*f* | 0.0000 | 0.3551 | 0.4371 |
| 0 | $C_6$:*Cmcm* | 5.9354 | 6.3121 | 2.4675 | C1 4*c* | 0.0000 | 0.5716 | 0.2500 |
| | (63) | 90 | 90 | 90 | C2 8*g* | 0.2949 | 0.2163 | 0.2500 |

**Supplementary Table S2.** The bond lengths and bond angle of carbon nanofoam ($C_6$, space group *Cmcm*), *Pmmn*, *Cmcm* phases of compressed $CaC_6$ compared to experimental data of graphite and diamond.

| Structure | Density(g/cm$^3$) | Bond length (Å) | | | Bond angle ($^0$) |
|---|---|---|---|---|---|
| Graphite | 2.27 | $sp^2$-$sp^2$ | 1.421 | $sp^2$-$sp^2$-$sp^2$ | 120.00 |
| diamond | 3.54 | $sp^3$-$sp^3$ | 1.545 | $sp^3$-$sp^3$-$sp^3$ | 109.47 |
| | | | 0 GPa | | |
| nanofoam | 2.589 | $sp^2$-$sp^2$ | 1.410 | $sp^2$-$sp^3$-$sp^2$ | 106.24 |
| $C_6$ (*Cmcm*) | | $sp^2$-$sp^3$ | 1.522 | $sp^3$-$sp^3$-$sp^3$ | 107.55 |
| | | $sp^3$-$sp^3$ | 1.529 | $sp^3$-$sp^3$-$sp^2$ | 110.77 |
| | | | | $sp^3$-$sp^2$-$sp^2$ | 118.93 |
| | | | | $sp^2$-$sp^2$-$sp^2$ | 120.11 |
| *Pmmn* | 3.499 | $sp^2$-$sp^2$ | 1.470,1.513 | $sp^2$-$sp^3$-$sp^2$ | 101.70,112.70 |
| | | $sp^2$-$sp^3$ | 1.582,1.620 | $sp^3$-$sp^3$-$sp^3$ | 107.43 |
| | | $sp^3$-$sp^3$ | 1.596 | $sp^3$-$sp^3$-$sp^2$ | 109.14,111.94 |
| | | | | $sp^3$-$sp^2$-$sp^2$ | 117.00,118.73 |
| | | | | $sp^2$-$sp^2$-$sp^2$ | 116.46,122.24 |
| | | | 39 GPa | | |
| *Pmmn* | 3.914 | $sp^2$-$sp^2$ | 1.426,1.467 | $sp^2$-$sp^3$-$sp^2$ | 101.59,113.92 |
| | | $sp^2$-$sp^3$ | 1.520,1.552 | $sp^3$-$sp^3$-$sp^3$ | 108.02 |
| | | $sp^3$-$sp^3$ | 1.538 | $sp^3$-$sp^3$-$sp^2$ | 108.69,111.80 |
| | | | | $sp^3$-$sp^2$-$sp^2$ | 117.07,119.01 |
| | | | | $sp^2$-$sp^2$-$sp^2$ | 116.05,121.50 |
| | | | 126 GPa | | |
| *Cmcm* | 4.788 | $sp^2$-$sp^2$ | 1.462 | $sp^3$-$sp^2$-$sp^2$ | 111.58 |
| | | $sp^2$-$sp^3$ | 1.461 | $sp^2$-$sp^3$-$sp^3$ | 111.58 |
| | | $sp^3$-$sp^3$ | 1.458,1.460<br>1.502,1.517 | $sp^3$-$sp^3$-$sp^3$ | 107.19, 109.41<br>110.78, 111.06 |
| | | | | $sp^2$-$sp^3$-$sp^2$ | 109.26 |
| | | | | $sp^3$-$sp^2$-$sp^3$ | 109.26 |

[1] Kittel, C. *Introduction to solid state physics* (8th edition, 2004).

**Supplementary Table S3.** The calculated values of the density of states at the Fermi level *N(0)*, phonon logarithmic average $\omega_{log}$, electron-phonon interaction $\lambda$, and superconducting transition temperature $T_c$ of $CaC_6$ for the *Pmmn* structure at different pressures. $\mu^*$ is the Coulomb pseudopotential parameter.

| **Space group** | ***P*** **（GPa）** | ***N(0)*** **（/Ry）** | $\omega_{log}$ **(*K*)** | $\lambda$ | $T_c$ **($\mu^*$=0.11)** | $T_c$ **($\mu^*$=0.115)** | $T_c$ **($\mu^*$=0.12)** |
|---|---|---|---|---|---|---|---|
| *Pmmn* | 39 | 15.645 | 642 | 0.445 | 3.87 | 3.48 | 3.12 |
| | 51 | 15.58 | 663 | 0.587 | 12.7 | 11.9 | 11.2 |
| | 78 | 15.378 | 623 | 0.638 | 15.4 | 14.7 | 13.9 |
| | 117 | 14.830 | 728 | 0.461 | 5.23 | 4.74 | 4.28 |

# Figure captions

**Supplementary Fig. S1. Projected density of states of *Pmmn* structure at phase transition pressure.** One can see that there is strong hybridization between Ca-*d* electrons and *p* electrons of C3 and C4 (forming $sp^2$ hybridized zigzag chains along y-axis direction). $sp^3$ hybridized C1 and C2 have very little contribution to Fermi level because of their saturated chemical bonds (see also Fig. S3).

**Supplementary Fig. S2. Projected density of states of *Cmcm* structure at phase transition pressure.** Weak hybridization between Ca-*d* electrons and C-*p* electrons is observed at Fermi level. Pressure brings about *d* energy level move to valence bands, which does good to decrease the total energy of system so as to compensate pressure-induced energetic increase, making it be favorable one energetically.

**Supplementary Fig. S3. Electronic local functional (ELF) and structural schematic diagram for *Pmmn* and *Cmcm* phases at phase transitional pressure.** Electronic local functional (ELF)[2] for *Pmmn* structure (a), nanofoam schematic diagram constructed by carbon atoms in *Pmmn* phase, centered with Ca ion chains (b) (unit: Å), Cmcm structure along (100) direction (c), and ELF for *Cmcm* structure (d) and (e). In (b) and (c), inequivalent carbon atoms depicted using different color balls, and calcium atoms shown using green balls. For *Pmmn* structure at 39 GPa, $sp^2$ were connected by $sp^3$ with C-C chemical bonding (length is 1.552 or 1.520 Å). Along y-axis direction, for $sp^2$ carbons, there are two types of C-C bonding with different lengths in zigzag chain (1.467 and 1.426 Å). While for $sp^3$ carbons, the bonding length in zigzag chains along y direction is 1.538 Å. For *Cmcm* structure at 126 GPa, the bonding length could be seen in Table S1.

**Supplementary Fig. S4. Phonon dispersion of *Pmmn* phase at zero pressure obtained using Phonopy code.** Obviously, it is stable dynamically.

**Supplementary Fig. S5. Phonon dispersion of *Cmcm* carbon nanoporous (appeared in phase III) at zero pressure obtained using Phonopy code[3].**

**Supplementary Fig. S6. At zero GPa, band structure of carbon foam (space group *Cmcm*) obtained by removing Ca atoms of phase III (space group, *Pmmn*).** The band gap is about 0.49 eV.

**Supplementary Fig S7. Four types of nanoform structures of intercalation compounds under compression.** $LiC_6$(a), $CaC_6$ (b), and $KC_8$ (c and d).

**Supplementary Fig S8. Total density of states (TDOS) for R-3m at ambient pressure, C222, Pmmn, and Cmcm phases at phase transition pressure.** Obviously, pressure leads to more expanded electronic distribution compared to that of *R-3m*, which leads to lower TDOS in *C222* and *Cmcm*. However, *Pmmn* phase has comparative TDOS with that of *R-3m* phase.

**Supplementary Fig S9. Phonon spectrum of three high pressure phases for $CaC_6$ at cold pressure calculated using Phonopy code.** There are soft modes in peculiar direction for *Pmmn* and *Cmcm* phases.

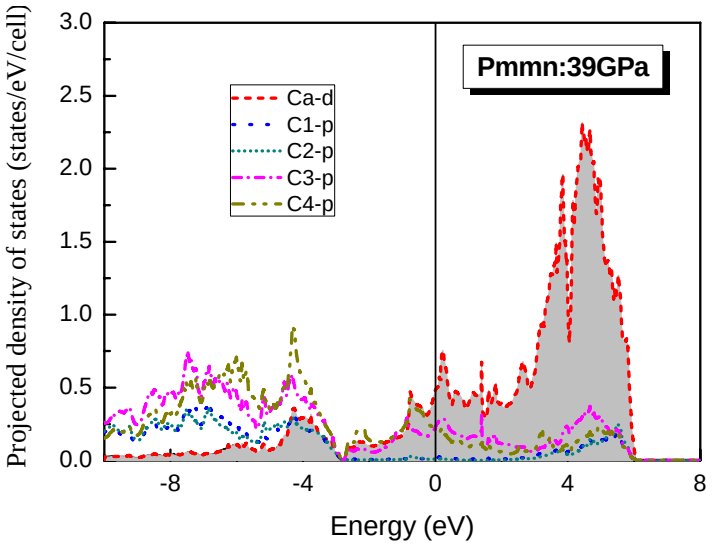


**Supplementary Fig. S1.** Projected density of states of Pmmn structure at phase transition pressure. One can see that there is strong hybridization between Ca-*d* electrons and *p* electrons of C3 and C4 (forming $sp^2$ hybridized zigzag chains along y-axis direction). $sp^3$ hybridized C1 and C2 have very little contribution to Fermi level because of their saturated chemical bonds (see also Fig. S3).

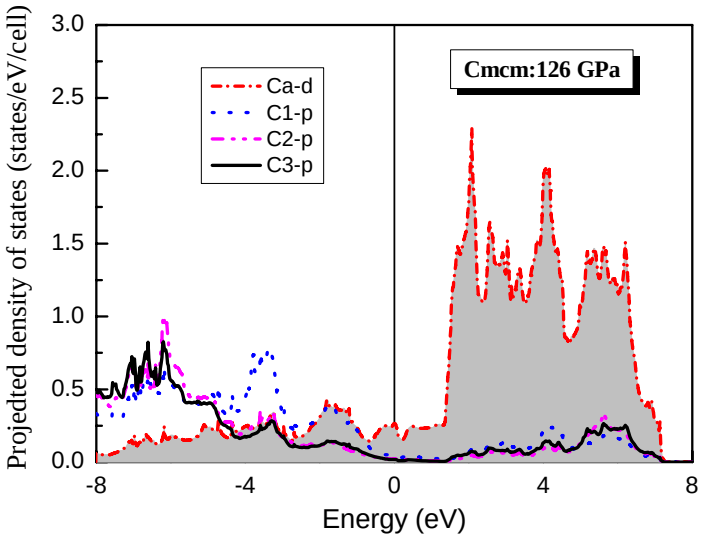


**Supplementary Fig. S2.** Projected density of states of *Cmcm* structure at phase transition pressure. Weak hybridization between Ca-*d* electrons and C-*p* electrons observed at Fermi level. Pressure brings about *d* energy level move to valence bands, which does good to decrease the total energy of system so as to compensate pressure-induced energetic increase, making it be favorable one energetically.

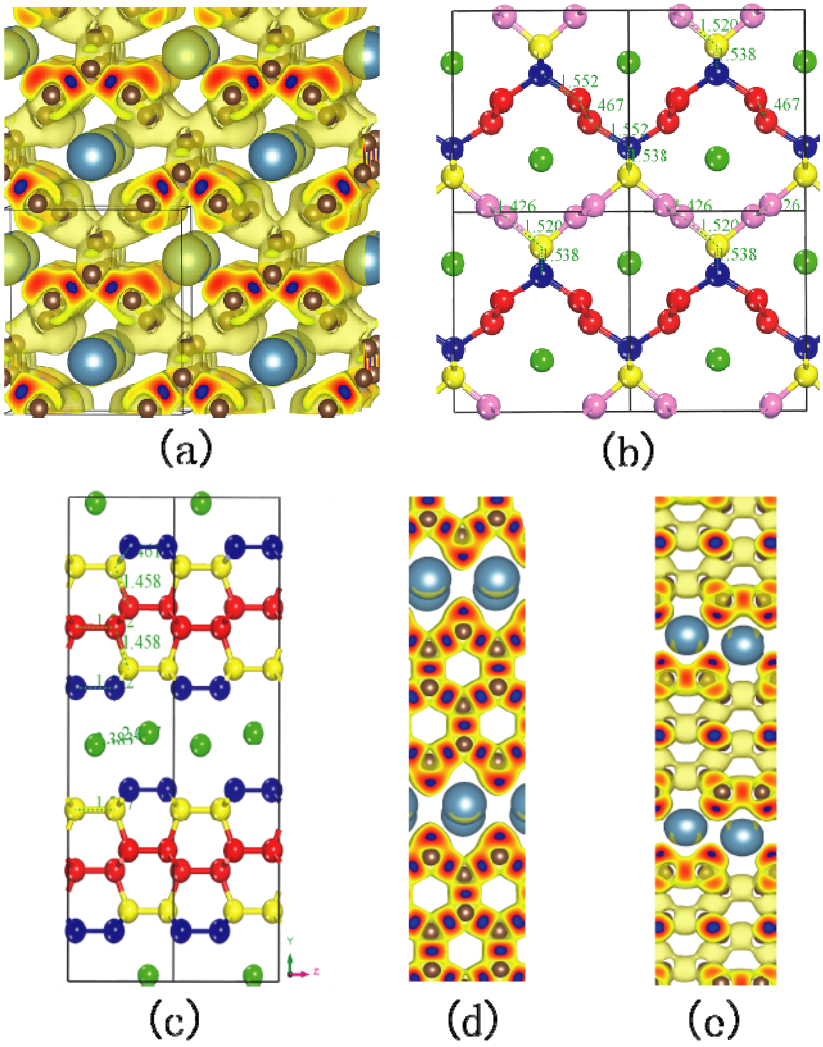


**Supplementary Fig.S3**. Electronic local functional (ELF)[2] for *Pmmn* structure (a), nanofoam schematic diagram constructed by carbon atoms in *Pmmn* phase, centered with Ca ion chains (b) (unit: Å), Cmcm structure along (100) direction (c), and ELF for *Cmcm* structure (d) and (e). In (b) and (c), inequivalent carbon atoms depicted using different color balls, and calcium atoms shown using green balls. For *Pmmn* structure at 39 GPa, $sp^2$ were connected by $sp^3$ with C-C chemical bonding (length is 1.552 or 1.520 Å). Along y-axis direction, for $sp^2$ carbons, there are two types of C-C bonding with different lengths in zigzag chain (1.467 and 1.426 Å). While for $sp^3$ carbons, the bonding length in zigzag chains along y direction is 1.538 Å. For *Cmcm* structure at 126 GPa, the bonding length could be seen in Table S1.

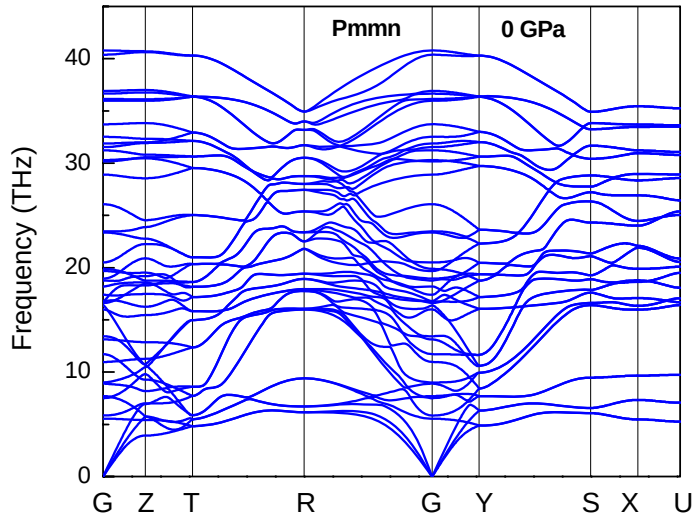


**Supplementary Fig S4.** Phonon dispersion of Pmmn phase at zero pressure obtained using Phonopy code. Obviously, it is stable dynamically.

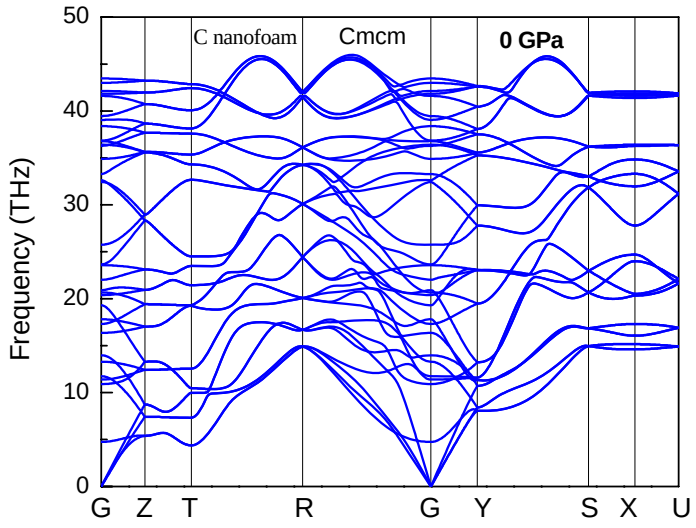


**Supplementary Fig. S5.** Phonon dispersion of Cmcm carbon nanoporous at zero pressure obtained using Phonopy code[3].

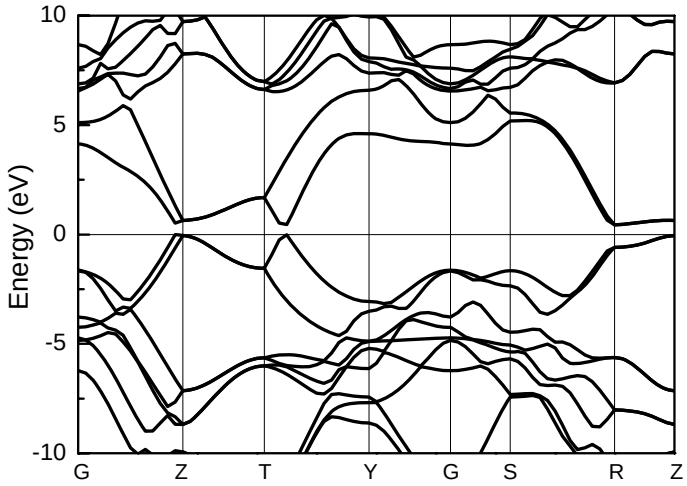


**Supplementary Fig. S6.** At zero GPa, band structure of carbon foam (space group *Cmcm*) obtained by removing Ca atoms of phase III (space group, *Pmmn*). The band gap is about 0.49 eV.

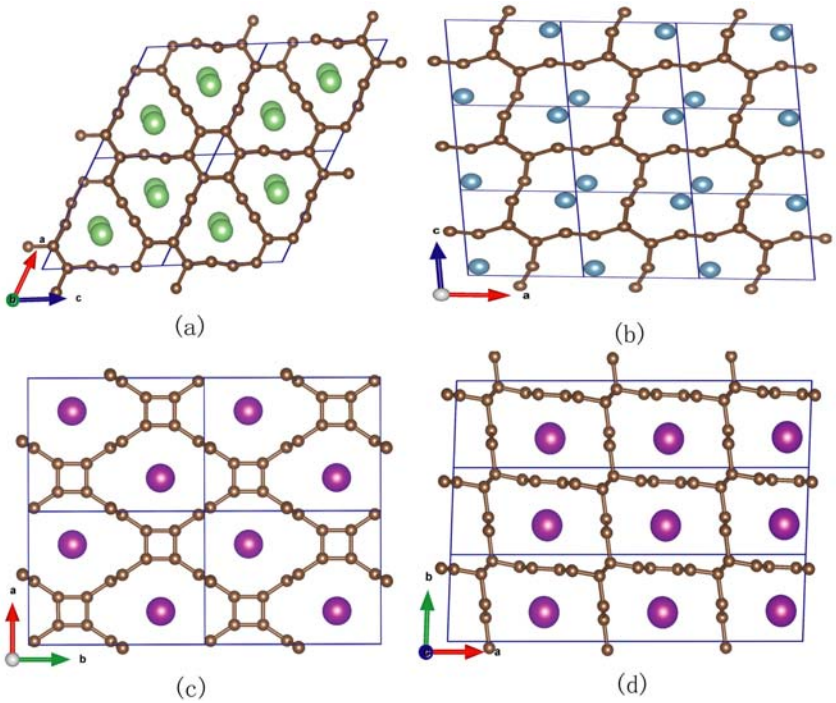


**Supplementary Fig. S7.** Four types of nanoform structures of intercalation compounds under compression. $LiC_6$(a), $CaC_6$ (b), and $KC_8$ (c and d).

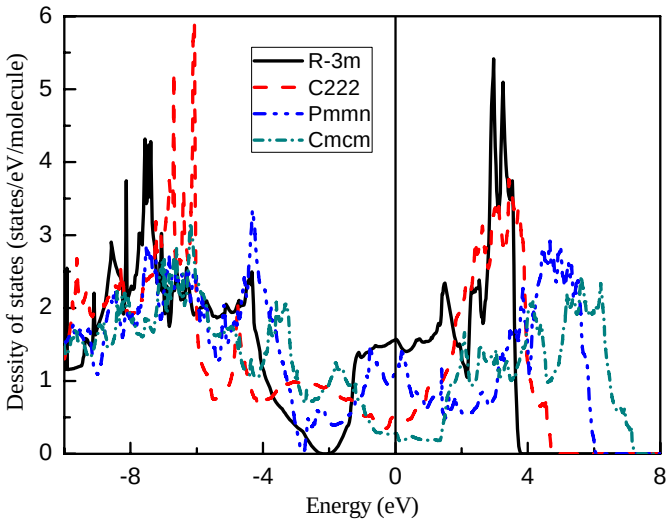


**Supplementary Fig S8.** Total density of states (TDOS) for *R-3m* at ambient pressure, *C222*, *Pmmn*, and *Cmcm* phases at phase transition pressure. Obviously, pressure leads to more expanded electronic distribution compared to that of *R-3m*, which leads to lower TDOS in *C222* and *Cmcm*. However, *Pmmn* phase has comparative TDOS with that of *R-3m* phase.

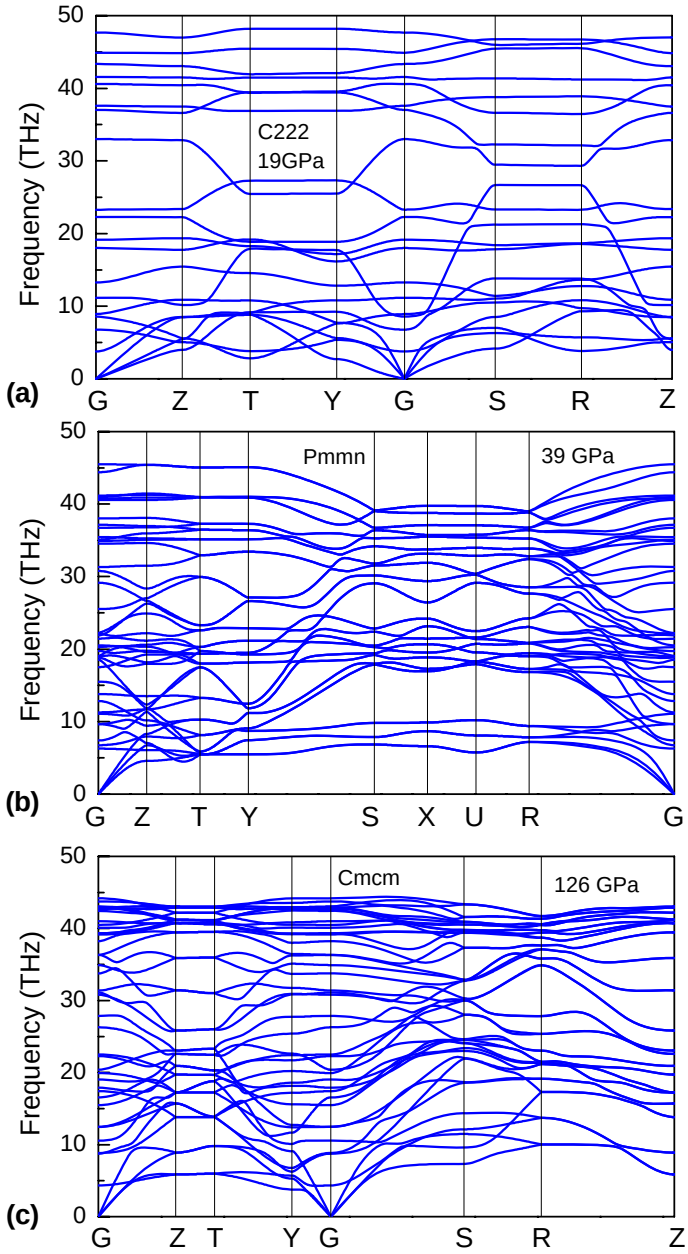


**Supplementary Fig. S9.** Phonon spectrum of three high pressure phases for $CaC_6$ at cold pressure calculated using Phonopy code. There are soft modes in peculiar direction for *Pmmn* and *Cmcm* phases.

## Reference:


1. Kittel C. *Introduction to solid state physics* (8th edition, 2004).
2. Momma K, and Izumi F (2011) VESTA 3 for three-dimensional visualization of crystal, volumetric and morphology data. *J. Appl. Crystallogr.* **44**, 1272-1276.
3. Togo A, Obe F, and Tanaka I (2008) First-principles calculations of the ferroelastic transition between rutile-type and $CaCl_2$-typre $SiO_2$ at high pressures. *Phys. Rev. B* **78**, 134106.